

New York, 1967), Vol. 20, p. 37.

<sup>14</sup>T. R. Werner, C. M. Falco, and I. K. Schuller, to be published.

<sup>15</sup>E. Abrahams, P. W. Anderson, D. C. Licciardello, and T. V. Ramakrishnan, Phys. Rev. Lett. **42**, 673 (1979).

<sup>16</sup>Y. Imry, J. Appl. Phys. **52**, 1817 (1981).

<sup>17</sup>B. L. Altshuler and A. G. Aronov, Zh. Eksp. Teor. Fiz. **77**, 2028 (1979) [Sov. Phys. JETP **50**, 968 (1979)].

<sup>18</sup>C. Kittel, *Introduction to Solid State Physics* (Wiley, New York, 1957), 2nd ed., p. 322. We are grateful to F. Blatt for pointing this out to us.

## Alloy Clustering in $\text{Ga}_{1-x}\text{Al}_x\text{As}$ Compound Semiconductors Grown by Molecular Beam Epitaxy

P. M. Petroff, A. Y. Cho, F. K. Reinhart, A. C. Gossard, and W. Wiegmann

*Bell Laboratories, Murray Hill, New Jersey 07974*

(Received 2 October 1981)

Direct evidence of alloy clustering in the  $\text{Ga}_{1-x}\text{Al}_x\text{As}$  alloy system is presented. Clustering is observed *only* on the nonpolar surface of GaAs. An exchange reaction model is proposed to account for the existence of a surface-orientation-dependent miscibility gap for this alloy system.

PACS numbers: 68.20.+t, 68.45.-v, 68.55.+b, 73.40.Lq

Alloy clustering in compound semiconductors has recently been suggested to explain the photoluminescence features of GaAs- $\text{Ga}_{1-x}\text{Al}_x\text{As}$  multi-quantum-well lasers grown by metal-organic vapor deposition.<sup>1</sup> The coexistence of two solid phases with different compositions necessary for defining clustering is very surprising for this alloy system since thermodynamic calculations<sup>2</sup> do not indicate a miscibility gap. However, computed phase diagrams only deal with thermodynamic properties of the bulk crystal. In the case of solid solutions formed by epitaxy at a vacuum-crystal surface, it might be expected that different thermodynamic equilibria exist for each different crystal surface and that these equilibria will differ with environment. The details of surface thermodynamics are not well enough understood to compute a "surface phase diagram" which takes into account the effects of surface reconstruction, the possibility of exchange reactions, and surface diffusion kinetics. However, crystal growth techniques such as molecular beam epitaxy (MBE)<sup>3</sup> offer the possibility of measuring experimentally some features of the surface phase diagram under controlled conditions. In this Letter we report the first evidence of a surface-orientation-dependent phase diagram for the  $\text{Ga}_{1-x}\text{Al}_x\text{As}$  alloy system grown by MBE. A miscibility gap is reported and the structure and composition in the solid solution suggest the existence of a spinodal reaction.

$\text{Ga}_{1-x}\text{Al}_x\text{As}$  ( $0.15 \leq x \leq 0.5$ ) epitaxial layers

have been deposited by MBE<sup>3,4</sup> at a temperature  $T_s = 600^\circ\text{C}$ , under growth conditions that would be As stabilized for a (100) growth. The GaAs substrate orientation was (110) for some depositions and for others  $\pm 2^\circ$  vicinally oriented from [110] with tilt axis parallel to the  $[\bar{1}10]$  direction. These vicinally oriented substrates contain surface steps with ledges parallel to  $[\bar{1}10]$  which are terminated either by Ga or As bonds. Typical growth rates are  $1 \mu\text{m/h}$ . The substrate preparation prior to the MBE deposition consisted of a standard bromine methanol etching and heating in UHV at a temperature of  $650^\circ\text{C}$  to remove the remaining oxide. The surface reconstruction of the (110) surface observed by reflection high-energy electron diffraction was  $(1 \times 1)$ . It has been established by ultraviolet photospectroscopy<sup>5</sup> and theoretical calculations<sup>6</sup> that surface relaxation of the outer layer takes place in such a way that the As moves out by  $0.2 \text{ \AA}$  and the Ga moves in by  $0.45 \text{ \AA}$ . The total displacement is  $0.65 \text{ \AA}$  for atoms on the surface, but it is expected to be more important at the steps for the vicinally oriented (110) surface.

In addition,  $\text{Ga}_{1-x}\text{Al}_x\text{As}$  depositions on (100)-oriented GaAs substrates were performed. For these (100)-oriented substrates and films the reconstructed surface was  $C(2 \times 8)$ .  $\text{Ga}_{1-x}\text{Al}_x\text{As}$  films were also deposited on (110) GaAs substrates by liquid-phase epitaxy (LPE)<sup>2</sup> using the standard graphite crucible process. The growth rate for these films was  $\geq 10 \mu\text{m/h}$  and the growth

temperature was either 650 or 800 °C. The deposited layers with thicknesses  $\geq 1 \mu\text{m}$  were examined by photoluminescence, low-temperature cathodoluminescence (CL), and transmission electron microscopy (TEM). Two types of TEM samples were prepared. The first type was prepared by selective etching of the substrate. With these samples, the electron beam is parallel to the MBE film growth axis. The second type was prepared for cross-sectional analysis of the layers. In the cross-section samples, the electron beam is parallel to the  $\text{Ga}_{1-x}\text{Al}_x\text{As}$ -GaAs interface. The TEM analysis is carried out using 200-keV electrons and standard kinematical and dynamical diffraction contrast imaging techniques. Chemical information was obtained by using a previously described dark-field forbidden-reflection contrast technique.<sup>7</sup> The chemical sensitivity of this technique to changes in the Al composition,  $x$ , was optimized by using the thinnest section of the sample and is estimated at  $\sim \pm 5\%$  variations of  $x$  when imaging the sample under kinematical diffraction conditions.<sup>8</sup> The spatial resolution of this forbidden-reflection dark-field technique was estimated to be  $\sim 10 \text{ \AA}$ . The low-temperature (20-K) CL spectral analysis is carried out with 100-keV electrons. Localized spectral information from  $1 \times 1 \mu\text{m}^2$  area as well as CL monochromatic micrographs is obtained by using a previously described CL-scanning-TEM instrument.<sup>9</sup>

Smooth  $\text{Ga}_{1-x}\text{Al}_x\text{As}$  epitaxial films are observed on (100) GaAs substrates and on the vicinally oriented (110) GaAs with As bonds at the steps. The (110)-oriented and the vicinally oriented (110) GaAs surfaces with Ga at the steps yield epitaxial films with rough surfaces.

The forbidden-reflection dark-field micrographs of cross-section samples for the MBE films (Fig. 1) grown under identical conditions on (110)- and (100)-oriented substrates show dramatic differences. In Fig. 1(a) the (110)-oriented GaAs substrate produces a dark contrast area and the  $\text{Ga}_{0.75}\text{Al}_{0.25}\text{As}$  layer exhibits quasiperiodic variations in the (200) diffracted intensity. The contrast conditions are such that the larger the Al content, the brighter the area. The platelike regions of the film with varying Al compositions have thicknesses ranging from 15 to  $\approx 300 \text{ \AA}$  and extend over  $\approx 1\text{-}\mu\text{m}$  areas. Their orientation is not always (110), and small deviations from the (110) orientation are indicated in Fig. 1(b). The diffraction pattern in Fig. 1(a) indicates the single-crystal character of the film. The  $\text{Ga}_{1-x}\text{Al}_x\text{As}$

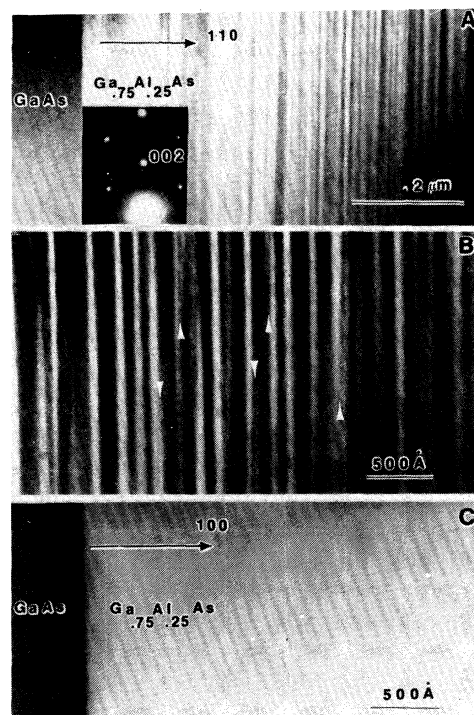


FIG. 1. (a) Dark-field transmission electron micrograph of a cross section through a  $\text{Ga}_{0.75}\text{Al}_{0.25}\text{As}$  film grown on a (110) GaAs substrate. The dark region on the left is the GaAs substrate. The dark and light areas in the  $\text{Ga}_{0.75}\text{Al}_{0.25}\text{As}$  film correspond to areas with varying Al content. The diffraction pattern of the epitaxial film indicates the (200) Bragg diffraction condition chosen for imaging. (b) Dark-field transmission electron micrograph of the same sample as in (a). The imaging conditions are identical to those in (a). White arrows indicate deviations of the platelike  $\text{Ga}_{1-x}\text{Al}_x\text{As}$  regions from the (110) orientation. (c) Dark-field transmission electron micrograph of a cross section through a  $\text{Ga}_{0.75}\text{Al}_{0.25}\text{As}$  film grown on a (100) GaAs substrate. The contrast conditions are identical to those in (a) and (b).

clustering was also observed on the vicinally oriented (110) surfaces.

By contrast, the  $\text{Ga}_{0.75}\text{Al}_{0.25}\text{As}$  deposited on the (100) GaAs substrate and imaged under conditions identical to those in Figs. 1(a) and 1(b) exhibits a uniform contrast indicative of a uniform Al distribution throughout the MBE film [Fig. 1(c)]. Similarly the  $\text{Ga}_{0.75}\text{Al}_{0.25}\text{As}$  films deposited by LPE on (100) or (110) GaAs substrates at 650 or 800 °C do not show evidence of clustering. The sensitivity of the technique is limited to composition variations of  $\pm 5\%$  of  $x$  over a volume larger than  $10^3 \text{ \AA}^3$ .

The CL spectral analysis taken with the elec-

tron beam parallel to the growth axis is shown in Fig. 2 for the (100)- and (110)-oriented films. The narrow luminescence line originating from the  $\text{Ga}_{0.90}\text{Al}_{0.10}\text{As}$  (100)-oriented film is consistent with an absence of variations in the Al content in the probed volume (probe diameter  $\approx 500$  Å). The shoulder at 1.625 eV and the peak at 1.595 eV have been associated with impurity (C and Ge) bound excitons. The broad luminescence line originating from the  $\text{Ga}_{0.90}\text{Al}_{0.10}\text{As}$  (110)-oriented film is consistent with the existence of a wide range of  $\text{Ga}_{1-x}\text{Al}_x\text{As}$  compositions ( $0.03 \leq x \leq 0.15$ ) in the excited volume of material. The peak in the luminescence corresponds to the composition which was directly determined from the measurements of the deposited AlAs and GaAs. This result, together with the TEM analysis, gives clear evidence of Al clustering in the (110)  $\text{Ga}_{1-x}\text{Al}_x\text{As}$  system.

The appearance of quasiperiodic variations in the chemical composition resulting from the co-deposition of Ga, Al, and As on the GaAs (110) surface at 600 °C is to be contrasted with depositions on the GaAs (100) surface. For the (100) GaAs films deposited by MBE under *optimal* conditions, there is no evidence of clustering from either photoluminescence<sup>10</sup> or TEM<sup>11</sup> studies. Detailed TEM studies of the  $\text{Ga}_{1-x}\text{Al}_x\text{As}$ -GaAs interface indicate that it can be sharp to one atomic

planar spacing,<sup>11</sup> suggesting that on (100) surfaces, interdiffusion or exchange reactions<sup>12</sup> between Ga atoms and Al atoms on the surface are not likely to occur rapidly enough even at the high deposition temperature. The same observations hold for the polar ( $\bar{1}\bar{1}\bar{1}$ ) surfaces since bilayer superlattices of GaAs-AlAs<sup>13</sup> have been fabricated on ( $\bar{1}\bar{1}\bar{1}$ )-oriented GaAs.

The extremely small interdiffusion coefficient<sup>7</sup> between Ga and Al in  $\text{Ga}_{1-x}\text{Al}_x\text{As}$  and GaAs films ( $D \leq 10^{-19}$  cm<sup>2</sup> sec<sup>-1</sup> for  $T \leq 700$  °C) suggests that the clustering observed in the (110)  $\text{Ga}_{1-x}\text{Al}_x\text{As}$  films grown by MBE is not the result of a bulk interdiffusion but rather is associated with *surface* reactions and diffusion during the film growth. For this reason, exchange reactions<sup>12</sup> which have been recently investigated<sup>5,6,14,15</sup> for Al or Ga deposited on GaAs or AlAs provide a useful basis for developing a model which could explain clustering. The exchange reaction on the (110) surface should be favored by the nonpolar character of this surface. The Gibbs free energy of the solid solution *at the surface* will be the sum of the intrinsic Gibbs free energy of the bulk solid solution (which may be computed with reasonable accuracy) and two extrinsic terms associated with the surface, namely the lattice misfit strain energy and the exchange reaction energy. The misfit strain has been measured for the  $\text{Ga}_{1-x}\text{Al}_x\text{As}$  solid solution<sup>16</sup> and is small ( $3 \times 10^{-4}$ ) at the growth temperature. The misfit strain is maximum for the (100) surfaces and decreases for (110) or (111) surfaces. Thus the exchange reaction energy contribution to the extrinsic Gibbs free energy appears to be the most important of the two. This contribution cannot presently be computed but we propose that changes in the Gibbs free energy introduced by the exchange reaction result in a miscibility gap in the  $\text{Ga}_{1-x}\text{Al}_x\text{As}$  phase diagram. The quasiperiodic variations in the  $\text{Ga}_{1-x}\text{Al}_x\text{As}$  composition for the (110)-oriented films should be a consequence of this miscibility gap and the deposition kinetics as the miscibility gap introduces a constraint in the possible compositions of the solid solution both on the growing surface and in the growth direction. Impurity pinning<sup>17</sup> is likely to affect the size of the  $\text{Ga}_{1-x}\text{Al}_x\text{As}$  islands of various composition by controlling the lateral growth of the atomic layers. Some evidence of this effect is seen in Fig. 1(b), where deviations in the compositional layering from the (110) orientation are indicated. The effects of the deposition kinetics are seen in the results of LPE-grown  $\text{Ga}_{1-x}\text{Al}_x\text{As}$  films deposited on (110) surfaces. These films

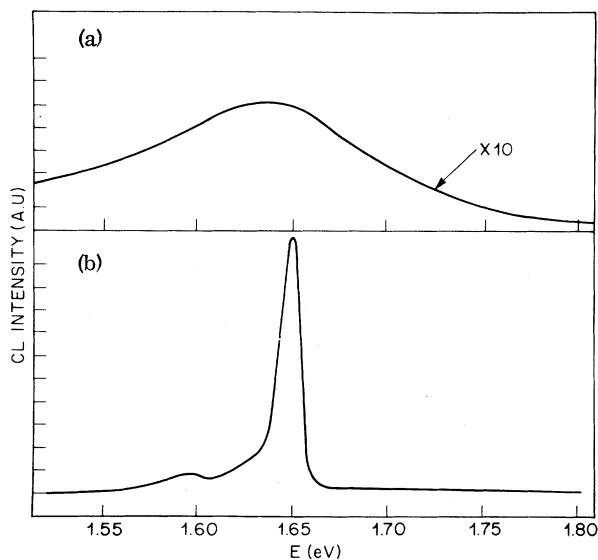


FIG. 2. (a) A low-temperature ( $T = 25$  K) cathodoluminescence (CL) spectrum of a  $\text{Ga}_{0.90}\text{Al}_{0.10}\text{As}$  film grown on a (110) GaAs substrate. (b) CL spectrum ( $T = 25$  K) of a  $\text{Ga}_{0.89}\text{Al}_{0.11}\text{As}$  film grown on a (100) GaAs substrate.

do not exhibit alloy clustering. Two possible reasons may account for the difference between the LPE and MBE growth. First, the LPE growth rates are 10 to 100 times more rapid than the MBE growth rates. Second, the LPE growth is essentially an equilibrium growth situation while in the MBE growth, the Al partial pressure is far above the equilibrium pressure value at the growth temperature. The difference may in fact provide an additional driving force for the exchange reaction and the phase separation.

The exchange-reaction-induced miscibility gap in the MBE-grown  $\text{Ga}_{1-x}\text{Al}_x\text{As}$  films could well result in a spinodal-type reaction which is characterized by a periodic variation in the solid solution composition.<sup>18</sup> This type of surface spinodal reaction which is of course controlled by diffusion at the surface could well be present in other semiconductor systems.<sup>19</sup>

The authors wish to thank M. B. Panish and J. C. Phillips for fruitful discussions, R. A. Logan for the LPE growth of the  $\text{Ga}_{1-x}\text{Al}_x\text{As}$  layers, and J. J. LePore for the sample preparation.

<sup>1</sup>N. Holonyak, Jr., W. D. Laidig, B. A. Vojcek, K. Hess, J. J. Coleman, P. D. Dapkus, and J. Bardeen, *Phys. Rev. Lett.* **45**, 1703 (1980).

<sup>2</sup>H. C. Casey, Jr., and M. B. Panish, *Heterostructure*

*Lasers* (Academic, New York, 1978), p. 71.

<sup>3</sup>A. Y. Cho, *J. Vac. Sci. Technol.* **16**, 275 (1979).

<sup>4</sup>K. Ploog, *Crystals: Growth, Properties and Applications* (Springer, Berlin, 1980), p. 73.

<sup>5</sup>R. Z. Bachrach, R. S. Bauer, P. Chiaradia, and G. V. Hansson, *J. Vac. Sci. Technol.* **19**, 335 (1981).

<sup>6</sup>C. B. Duke, A. Paton, R. J. Meyer, L. J. Brillson, A. Kahn, D. Kanani, J. Carelli, J. Z. Yeh, G. Margaritando, and A. D. Katnani, *Phys. Rev. Lett.* **46**, 440 (1981).

<sup>7</sup>P. M. Petroff, *J. Vac. Sci. Technol.* **14**, 973 (1977).

<sup>8</sup>A. Olsen, J. C. M. Spence, and P. M. Petroff, in *EMSA Proceedings—1980*, edited by G. W. Bailey (Claitor's Publishing, Baton Rouge, 1980), p. 120.

<sup>9</sup>P. M. Petroff, D. V. Lang, J. L. Strudel, and R. A. Logan, *Scanning Electron Microscopy* (SEM Inc., AMF O'Hare, Ill., 1978), Vol. 1, p. 325.

<sup>10</sup>R. C. Miller and W. T. Tsang, *Appl. Phys. Lett.* **39**, 334 (1981).

<sup>11</sup>P. M. Petroff, A. C. Gossard, W. Wiegmann, and A. Savage, *J. Cryst. Growth* **44**, 5 (1978).

<sup>12</sup>J. C. Phillips, *J. Vac. Sci. Technol.* **11**, 947 (1974).

<sup>13</sup>P. M. Petroff, A. C. Gossard, W. Wiegmann, unpublished.

<sup>14</sup>A. Huijser, J. VanLaar, and T. L. VanRooy, *Surf. Sci.* **102**, 264 (1981).

<sup>15</sup>G. Landgren and R. Ludeke, *Solid State Commun.* **37**, 127 (1981).

<sup>16</sup>G. A. Rozgonyi, P. M. Petroff, and M. B. Panish, *J. Cryst. Growth* **27**, 106 (1974).

<sup>17</sup>J. C. Phillips, *J. Vac. Sci. Technol.* **19**, 545 (1981).

<sup>18</sup>J. W. Cahn, *Acta Metall.* **9**, 795 (1961).

<sup>19</sup>P. M. Petroff, A. C. Gossard, and W. Wiegmann, *J. Cryst. Growth* **46**, 172 (1979).

## Mechanical Measurements on Free-Standing Films of Smectic Liquid-Crystal Phases

R. Pindak, W. O. Sprenger, D. J. Bishop, D. D. Osheroff, and J. W. Goodby

*Bell Laboratories, Murray Hill, New Jersey 07974*

(Received 30 September 1981)

Shear mechanical properties have been measured for free-standing films of the liquid crystal *n*-hexyl 4'-*n*-pentyloxybiphenyl-4-carboxylate (65OBC) in its stacked-hexatic *B* phase. The smectic-*I* phases of (+)-4-(2'-methylbutyl)phenyl 4'-*n*-nonyloxybiphenyl-4-carboxylate and (-)-2-methylbutyl 4-(4'-*n*-decyloxybenzylideneamino) cinnamate (DOBAMBC) were also studied. Unlike the crystal *B* phase, none of these phases exhibited an in-plane shear modulus. Enhanced crystalline surface ordering was observed in 65OBC.

PAC numbers: 61.30.Eb, 62.20.Dc

Several techniques have been developed to study the shear mechanical properties of free-standing smectic liquid-crystal films.<sup>1-4</sup> These films, which can be varied in thickness from two to

hundreds of molecular layers, provide good model systems for observing the evolution from two to three dimensions. The mechanical techniques were first used to study the *B* phase in free-

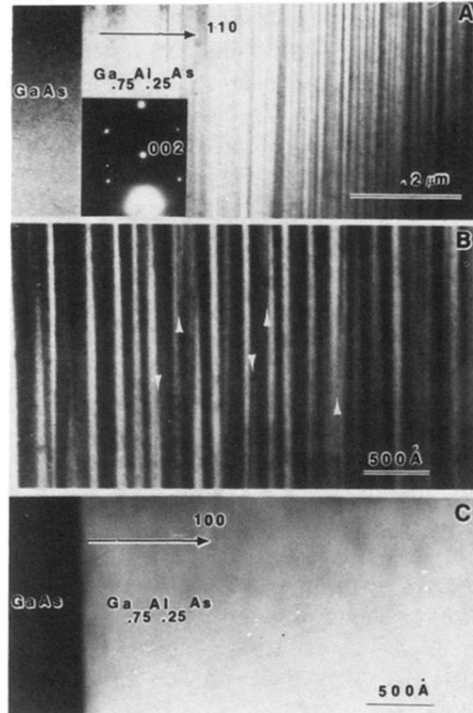


FIG. 1. (a) Dark-field transmission electron micrograph of a cross section through a Ga<sub>0.75</sub>Al<sub>0.25</sub>As film grown on a (110) GaAs substrate. The dark region on the left is the GaAs substrate. The dark and light areas in the Ga<sub>0.75</sub>Al<sub>0.25</sub>As film correspond to areas with varying Al content. The diffraction pattern of the epitaxial film indicates the (200) Bragg diffraction condition chosen for imaging. (b) Dark-field transmission electron micrograph of the same sample as in (a). The imaging conditions are identical to those in (a). White arrows indicate deviations of the platelike Ga<sub>1-x</sub>Al<sub>x</sub>As regions from the (110) orientation. (c) Dark-field transmission electron micrograph of a cross section through a Ga<sub>0.75</sub>Al<sub>0.25</sub>As film grown on a (100) GaAs substrate. The contrast conditions are identical to those in (a) and (b).